HHS Public Access

Author manuscript

Orthod Craniofac Res. Author manuscript; available in PMC 2016 April 01.

Published in final edited form as:

Orthod Craniofac Res. 2015 April ; 18(0 1): 196–206. doi:10.1111/ocr.12080.

The Effects of Tissue-Nonspecific Alkaline Phosphatase Gene Therapy on Craniosynostosis and Craniofacial Morphology in the FGFR2$^{C342Y/+}$ Mouse Model of Crouzon Craniosynostosis

E Wang[1], **HK Nam**[1], **J Liu**[1], and **NE Hatch**[1]

[1]Department of Orthodontics and Pediatric Dentistry, School of Dentistry, University of Michigan, Ann Arbor, MI, USA

Abstract

Objectives—Craniosynostosis, the premature fusion of cranial bones, has traditionally been described as a disease of increased bone mineralization. However, multiple mouse models of craniosynostosis display craniosynostosis simultaneously with diminished cranial bone volume and/or density. We propose an alternative hypothesis that craniosynostosis results from abnormal tissue mineralization through the downregulation of tissue-nonspecific alkaline phosphatase (TNAP) enzyme downstream of activating mutations in FGFRs.

Material & Methods—Neonatal Crouzon (FGFR$^{C342Y/+}$) and wild type (FGFR$^{+/+}$) mice were injected with lentivirus to deliver a recombinant form of TNAP. Mice were sacrificed at four weeks post-natal. Serum was collected to test for alkaline phosphatase (AP), phosphorus, and calcium levels. Craniofacial bone fusion and morphology was assessed by micro-computed tomography.

Results—Injection with the TNAP lentivirus significantly increased serum AP levels (increased serum AP levels are indicative of efficient transduction and production of the recombinant protein), but results were variable and dependent upon viral lot and the litter of mice injected. Morphologic analysis revealed craniofacial form differences for inferior surface (p=.023) and cranial height (p=.014) regions between TNAP lentivirus injected and vehicle-injected Crouzon mice. With each unit increase in AP level, the odds of lambdoid suture fusion decreased by 84.2% and these results came close to statistical significance (p=.068).

Conclusion—These results suggest that TNAP deficiency may mediate FGFR2-associated craniosynostosis. Future studies should incorporate injection of recombinant TNAP protein, to avoid potential side effects and variable efficacy of lentiviral gene delivery.

Keywords

craniofacial; craniosynostosis; bone; mineralization; mouse model

Correspondence to: Nan Hatch, Department of Orthodontics and Pediatric Dentistry, 1011 N University Avenue, University of Michigan, Ann Arbor, MI, USA 48109-1078, nhatch@umich.edu.

INTRODUCTION

Craniosynostosis is a craniofacial anomaly characterized by the premature fusion of cranial bones. The only treatment for craniosynostosis is surgery, which aims to relieve elevated intracranial pressure and normalize skull and facial shapes (1–3). Specific genetic mutations occur in association with craniosynostosis, including mutations in the Fibroblast Growth Factor receptor (FGFR) gene family (4). However, the precise molecular mechanism by which these mutations cause craniosynostosis remains unknown.

Studies of mouse models of craniosynostosis reveal the potential error in oversimplifying the mechanism of craniosynostosis as being a disorder of excess cranial bone formation and/or mineralization. That is, previous studies of the $FGFR2^{C342Y/+}$ mouse model of Crouzon syndrome showed that these mice exhibit craniosynostosis with decreased cranial bone volume and density (5–7). Similarly, previous investigations showed that the $FGFR2^{S250W/+}$ mouse model of Apert syndrome exhibits craniosynostosis with diminished cranial bone thickness and formation (8), while the $FGFR2^{P253R/+}$ mouse model of Apert syndrome exhibits craniosynostosis with retarded endochondral bone growth and ossification (9). In addition, study of the $FGFR3^{P244R/+}$ mouse model of Muenke syndrome demonstrated that these mice exhibit craniosynostosis with delayed calvarial ossification and diminished bone density (10). Together, these results highlight the possibility that the pathogenesis of craniosynostosis may reflect an as yet unknown mechanism involving imbalanced bone and suture mineralization.

Previous studies have shown that inorganic phosphate (Pi) to pyrophosphate (PPi) concentration ratios, as mediated by ectonucleotide pyrophosphatase/phosphodiesterase 1 (Enpp1) and tissue nonspecific alkaline phosphatase (TNAP), control tissue mineralization (11). Enpp1 is the primary enzymatic generator of PPi by bone forming cells (12). TNAP hydrolyzes PPi to Pi and TNAP activity is essential for hydroxyapatite crystal formation (13, 14). PPi inhibits hydroxyapatite crystal deposition (15), but also serves as an essential source of Pi to promote mineralization after hydrolysis by TNAP (13, 14). Additionally, while physiologic PPi levels inhibit hydroxyapatite deposition, excess PPi can promote the pathologic deposition of non-apatitic mineral crystals in soft tissues (16–18). PPi and Pi can also influence tissue mineralization by altering osteoblastic gene expression and behavior (19–21). Notably, craniosynostosis occurs at a high incidence in infants with hypophosphatasia due to inactivating mutations in the gene for TNAP (22, 23). These patients have severely deficient bone mineralization (24, 25).

We propose that altered expression of enzymes involved in PPi metabolism, downstream of FGF signaling, could provide a molecular mechanism for the aberrant mineralization phenotype of FGFR-associated craniosynostosis. In support of this hypothesis, we previously showed that FGF signaling increases Enpp1 and inhibits TNAP expression and activity in calvarial osteoblasts (26, 27). Cells isolated from Crouzon $FGFR2^{C342Y/+}$ mice also exhibit diminished TNAP mRNA and enzyme activity levels (7). These data, combined with the clinical knowledge that craniosynostosis occurs at high rates in patients with deficient TNAP, support the idea that the pathogenesis of craniosynostosis involves diminished TNAP activity. To determine directly if diminished TNAP enzyme levels

precipitate FGFR2-associated craniosynostosis, in this study we injected mice that carry the Crouzon syndrome-associated FGFR2$^{C342Y/+}$ mutation, with lentivirus that allows for sustained expression of recombinant TNAP.

MATERIALS AND METHODS

FGFR2$^{C342Y/+}$ Mice

Animal procedures were performed according to the University of Michigan's Committee on Use and Care of Animals. Mice carrying the Crouzon syndrome FGFR2$^{C342Y/+}$ mutation on the BALB/c genetic background have a consistent craniofacial phenotype involving craniofacial shape changes and fusion of specific sutures (7). Genotyping of Crouzon (FGFR2$^{C342Y/+}$) and wild type (FGFR2$^{+/+}$) mice was performed as previously described (5). Briefly, DNA from tail digests was amplified by polymerase chain reaction using 5'-gagtaccatgctgactgcatgc-3' and 5'-ggagaggcatctctgtttcaagacc-3' primers. Genotypic ratios were as predicted. Litter sizes ranged from 5 to 10 pups per litter (avg = 7.5+/- 3 pups per litter). Pups were sacrificed at 4 weeks old for analysis. Blood was collected by aortic puncture. Body weight and length were measured.

Mineral-targeted TNAP Lentivirus and Injections

Mineral-targeted TNAP lentivirus was generously provided by Dr. Jose Luis Millán (Sanford-Burnham Medical Research Institute, La Jolla, CA). This lentivirus expresses a fusion protein containing TNAP enzyme fused at its C-terminal end to a constant region of the human IgG1 Fc domain and a deca-aspartate sequence (28). The deca-aspartate sequence targets the enzyme to hydroxyapatite (29).

In this study, five litters of mice (n=32 pups: 8 wild type male, 8 wild type female, 6 Crouzon male and 10 Crouzon female) were injected three days after birth with lentivirus (1.0×10^7 transforming units per mouse) via the jugular vein. Each litter was injected with a different viral lot/preparation. Four litters of mice (n=28 pups: 7 wild type male, 7 wild type female, 6 Crouzon male and 8 Crouzon female) were injected with an equivalent volume of sterile phosphate buffered saline (vehicle).

Serum Alkaline Phosphatase Activity, Phosphate and Calcium Analyses

Alkaline phosphatase activity (AP) serum levels were quantified by spectrophotometry, using a colorimetric reagent (Sigmafast, Sigma Aldrich Co. LLC., St. Louis, MO). Alkaline phosphatase activity units were calculated by comparison to a standard curve. Serum AP levels are indicative of efficient transduction and production of the recombinant TNAP protein (28).

Inorganic phosphate and calcium quantification was performed using commercially available kits (Inorganic Phorphorus Reagent Set, Calcium Reagent Set, Pointe Scientific, Inc., Canton, MI). Inorganic phosphorus (mg/dL) and calcium (mg/dL) levels were calculated by comparison to standard curves.

Micro-Computed Tomography (micro-CT)

Whole skulls were dissected and fixed in ethanol. Calvaria were embedded in 1% agarose and scanned using a micro-CT system (μCT100 Scanco Medical, Bassersdorf, Switzerland) at 18 μm voxel resolution. Scans were calibrated to the manufacturer's hydroxyapatite phantom.

Suture Fusion Assessment

Patency or fusion of craniofacial sutures was established by serial viewing of individual slices in the axial, sagittal and coronal planes throughout the entire length of the suture in question using micro-CT scans (Microview Version 2.1.2, GE Healthcare PreClinical Imaging, London, ON), as previously described (7). Fusion was verified by analysis of micro-CT scans by two independent reviewers. Sutures analyzed included the intersphenoidal suture (ISS), the spheno-occipital suture (SOS), the lambdoid suture and the sagittal suture. The coronal suture was not analyzed due to difficulty of clear visualization of this suture with the micro-CT equipment and/or software used.

Three-dimensional Craniofacial Morphological Analysis

Three-dimensional X, Y, Z coordinate data from thirty-three landmarks placed on micro-CT images of mouse skulls were used to assess quantitatively craniofacial form in this study, as previously described (Fig. 1; 7,30). Landmarks were placed using orthodontic imaging software (Dolphin Imaging 11.0, Dolphin Imaging and Management Solutions, Chatsworth, CA). Reliability of this method was previously reported (7). Landmark coordinate data were imported into analytic software (WinEDMA 1.0.1, Theodore Cole, University of Missouri, Kansas City, MO). This software uses three-dimensional coordinate data to quantify and compare forms between two sample populations by Euclidean distance matrix analysis (EDMA), which allows for an invariant statistical comparison of forms (32).

In this study, we compared Crouzon mice injected with the TNAP lentivirus (litters 1–4) with Crouzon mice injected with vehicle (litters 6–9). Litter 5 was not used for analysis since their serum alkaline phosphatase levels were comparable to vehicle injected mice, indicating lack of efficacy of the virus in these mice. Landmarks were grouped into regional subsets, due to the high number of landmarks used.

Statistical Analysis

Mice injected with the TNAP lentivirus displayed varying levels of AP enzyme activity, indicating variable efficacy of the virus. Therefore, logistic regression was used to model the log odds of the binary outcome of cranial suture or synchondrosis fusion. This statistical model allowed us to draw conclusions about the relationship between the level of AP enzyme activity and our ability to influence suture fusion, despite the variability in AP enzyme activity levels between mice. Linear regression was used to analyze the effect of the AP level, genotype and gender on continuous outcomes including body weight, body length, serum inorganic phosphorus and serum calcium levels.

RESULTS

Serum alkaline phosphatase activity

Injection with the lentivirus significantly increased serum alkaline phosphatase (AP) activity levels, when compared to vehicle injected mice (Fig. 2A). Vehicle injected wild type mice had a mean AP level of 0.05 ± 0.02 units; vehicle injected Crouzon mice had a mean level of 0.05 ± 0.01 units; TNAP lentivirus injected wild type mice had a mean AP level of 0.63 ± 0.49 units and TNAP lentivirus injected Crouzon mice had a mean AP level of 0.60 ± 0.46 units.

Despite injecting similar titers of virus, AP levels were variable and dependent upon the lot of virus/litter injected (Fig. 2B). Litter 1 had the highest AP activity, with an average level of 1.2 ± 0.27 units. Litter 2 had an average AP level of 0.79 ± 0.15 units, while litters 3 and 4 had even lower levels. Litter 3 had an average AP level of 0.27 ± 0.09 units and litter 4 had an average AP level of 0.30 ± 0.10 units. Litter 5 was injected with the lentivirus but showed AP activity similar to that seen in control mice (mean AP level was 0.07 ± 0.05 units). No differences between genotypes or genders were found.

Body weight and body length measurements

With every unit increase in AP activity, there was a decrease in body weight by 1.4 g for both Crouzon ($FGFR2^{C342Y/+}$) and wild type ($FGFR2^{+/+}$) mice (p=.004) (Table 1). Crouzon mice weighed on average 2.9 g less than wild type mice, regardless of AP level ($p < .0001$). The influence of AP level on body weight was the same for both wild type and Crouzon mice. The overall R^2 value was .519 (overall $p < .0001$) which means that the regression model model (including AP level, genotype and gender as variables) accounted for 51.9% of the variability in weight.

With every unit increase in AP level, there was a decrease in body length by 4.5 mm for both Crouzon and wild type mice ($p < .003$) (Table 1). Crouzon mice on average measure 6.5 mm less than wild type mice, regardless of AP level ($p < .0001$), and there is no statistically significant interaction between AP level and genotype. The overall R^2 value was .395 (overall $p < .0001$) which means that the regression model (including AP level, genotype and gender as variables) accounted for 39.5% of the variability in body length.

Serum inorganic phosphorus and calcium assays

Neither injection with the TNAP lentivirus, gender, nor genotype had a significant effect on serum phosphorus levels. Vehicle injected wild type mice had a mean serum inorganic phosphorous level of 10.2 ± 1.3 mg/dl; vehicle injected Crouzon mice had a mean serum inorganic phosphorous level of 10.3 ± 2.8 mg/dl; TNAP lentivirus injected wild type mice had a mean serum inorganic phosphorous level of 9.5 ± 1.2 mg/dl and TNAP lentivirus injected Crouzon mice had a mean serum inorganic phosphorous level of 9.3 ± 1.3 mg/dl. With every unit increase in AP level, there was an increase in serum inorganic phosphorous by 1.0 mg/dl for Crouzon and by 0.6 mg/dl for wild type mice, but these differences were not statistically significant (p=.10 for Crouzon, p=.24 for wild type). The corresponding R^2 values for Crouzon and wild-type mice were .094 and .050 respectively, which means that

the regression model (including AP level, genotype and gender as variables) accounted for only 9.4% and 5.0% of the variability in serum inorganic phosphate in Crouzon and wild type mice, respectively.

Injection with the TNAP lentivirus, gender, and genotype also did not significantly influence serum calcium levels. Vehicle injected wild type mice had a mean serum calcium level of 9.1 ± 0.4 mg/dl; vehicle injected Crouzon mice had a mean serum calcium level of 8.9 ± 0.5 mg/dl; TNAP lentivirus injected wild type mice had a mean serum calcium level of 8.6 ± 0.3 mg/dl and TNAP lentivirus injected Crouzon mice had a mean serum calcium level of 8.5 ± 0.4 mg/dl. With every unit increase in AP level, there was an increase in serum calcium by 0.4 mg/dl for Crouzon and by 0.1 mg/dl for wild type mice. While this increase was significant for Crouzon mice ($p < .05$ for Crouzon, $p=.72$ for wild type), regression analysis incorporating all three variables (AP level, gender and genotype) revealed a lack of significance ($p=.228$), demonstrating that AP level did not have a significantly effect on serum calcium. The corresponding R^2 values for Crouzon and wild-type mice were .135 and .005 respectively, which means that the regression model (including AP level, genotype and gender as variables) accounted for only 13.5% and 0.5% of the variability in serum inorganic phosphate in Crouzon and wild type mice, respectively.

Suture fusion

All Crouzon mice, regardless of treatment, exhibited fusion of the intersphenoidal synchondrosis (ISS). No wild type mice, regardless of treatment, exhibited fusion of the sagittal suture. The spheno-occipital synchondrosis (SOS) was fused in 28.6% of vehicle injected Crouzon mice and in 25.0% of TNAP lentivirus injected Crouzon mice. The lambdoid suture was fused in 61.9% of vehicle injected Crouzon mice and in 56.3% of TNAP lentivirus injected Crouzon mice (Fig. 3A).

Injection with the TNAP lentivirus resulted in higher expression levels in mouse litter 1 and litter 2, than in subsequent litters. When comparing these two litters of TNAP lentivirus injected mice with all vehicle injected mouse litters, the SOS was fused in 28.6% of vehicle injected Crouzon mice and in 14.3% of TNAP lentivirus injected Crouzon mice. The lambdoid suture was fused in 61.9% of vehicle injected Crouzon mice and in 28.6% of TNAP lentivirus injected Crouzon mice (Fig. 3B).

To account for the variable efficacy of injected virus, we next performed logistic regression analysis to assess the effect of AP level on suture fusion in Crouzon mice. For every unit increase in AP level, the odds of fusion of the SOS decreased by 41.7% (Table 2). However the p value did not reach significance ($p = 0.602$). For every unit increase in AP level, the odds of fusion of the lambdoid suture decreased by 84.2%. This result falls just short of significance ($p = 0.068$) (Table 2).

Morphological Analysis

The craniofacial subset comparisons that were significantly different between TNAP lentivirus injected and vehicle injected Crouzon mice were for the inferior surface ($p = 0.02$) and cranial vault vertical ($p = 0.01$) regions (Table 3). Skull vertical height dimensions were diminished in TNAP lentivirus injected Crouzon mice, when compared to vehicle injected

Crouzon mice (significant form estimate confidence intervals for landmarks 5–30, 5–28, 5–29, 4–28, 4–29). Skull transverse dimensions were also diminished in TNAP lentivirus injected Crouzon mice, when compared to vehicle injected Crouzon mice (significant form estimate confidence intervals for landmarks 24–25, 12–13).

DISCUSSION

This study describes effects of a TNAP lentivirus in Crouzon ($FGFR2^{C342Y/+}$) mice to assess its potential as a therapeutic drug for craniosynostosis. Ideally, such a drug would decrease the degree of suture fusion so as to minimize the craniofacial dysmorphology and intracranial pressure that can be caused by craniosynostosis. Over-expression of TNAP also tests our hypothesis that FGFR2 gain-of-function mutations suppress TNAP expression thereby causing abnormalities in craniofacial bone and suture mineralization. Previous studies have systemically overexpressed TNAP in mice and humans for the treatment of the skeletal hypomineralization seen in hypophosphatasia (28, 32–34). This is the first study to specifically analyze the craniofacial effects of TNAP.

Lentivirus is a useful form of drug provision because it requires only a single injection for sustained delivery, as the viral genome integrates into the host cell genome for stable expression of the encoded protein. Previous studies using this recombinant TNAP lentivirus achieved increased serum AP levels and significant reductions in long bone hypomineralization in the TNAP null mouse model of infantile hypophosphatasia, indicating that the virus is efficacious (28). In this study, TNAP lentivirus produced a significant increase in serum alkaline phosphatase levels compared to those of vehicle injected mice but the efficacy of the injection was variable, dependent upon the litter injected. This variability in AP level may be due to many factors including inaccurate titer of virus (each litter was injected with a different lot of virus), and variations in viral integration and replication within the host. The variation in AP level serendipitously allowed us to test a dose-response relationship between AP level and body weight, body size, craniosynostosis and craniofacial morphology using linear and logisitic regression analyses. A limitation of the regression analyses performed in this study is the small number of mice with high serum AP levels in lentiviral injected mice. Future studies should include injection of additional mice with virus in order to attain more mice with higher serum AP levels.

In this study, serum AP level had a diminishing effect on body weight and length regardless of gender or genotype, suggesting that the TNAP lentivirus had a negative effect on overall growth. Similar reductions in growth as reflected by body weight were reported upon injection of TNAP null mice with the TNAP lentivirus (28). Because injection with the same TNAP protein that is encoded in this lentivirus previously led to increased weight gain in injected mice (33), we suspect that the lentivirus itself in some manner inhibits body growth and weigth gain. Future studies should incorporate injection of the recombinant TNAP protein, to avoid both potential side effects and the variable efficacy of lentiviral delivery.

Suture fusion analysis was difficult, due to the small number of mice with high serum AP activity. When all lentivirus treated mice were grouped together, minimal differences in fusion of cranial sutures or cranial base synchondroses were seen. When TNAP virus

injected mice only with higher serum AP levels are compared with vehicle injectedmice, the incidence of lambdoid suture fusion decreased from 61.9% to 28.6% and the incidence of SOS fusion decreased from 28.6% to 14.3%. Logisitic regression showed that the odds of lamdoid suture fusion decreased by 84.2%. However, these results were not statistically significant (p=.068). Clearly, more mice injected with TNAP lentivirus and exhibiting high levels of AP activity are required to definitively show an effect of TNAP on craniosynostosis.

Crouzon mice on the BALB/c genetic strain are significantly different in craniofacial morphology than wild type mice (7). In this study, EDMA analysis was used to determine if the TNAP lentivirus altered the craniofacial form of injected Crouzon mice. Due to the large number of landmarks utilized, the craniofacial skeleton was divided into spacial regions. The inferior craniofacial surface and the cranial vault vertical regions were significantly different between TNAP lentivirus injected and vehicle injected mice. These results suggest that TNAP lentivirus treatment may rescue the craniofacial form of Crouzon mice. More specifically, it has been shown that skull width and height of Crouzon mice is increased when compared to that of wild type mice (6). EDMA results of this study revealed that vertical and transverse dimensions were diminished in TNAP lentivirus injected Crouzon mice when compared to vehicle injected Crouzon mice, suggesting the possibility that delivery of the recombinant TNAP enzyme rescues these abnormalities in shape. It is important to remember that this analysis was based upon mice grouped by treatment and, as previously stated, AP level varied to such an extent in treated mice that this grouping may not be able to detect fully the effects of the treatment on craniofacial form.

CONCLUSIONS

Lentiviral delivery of recombinant TNAP caused a decrease in overall growth of the mice compared to vehicle injected mice. EDMA analysis revealed that there were regional craniofacial form effects of the TNAP lentivirus injection compared to vehicle injection treatments. The virus injection treatment also appeared to diminish fusion of the lambdoid suture, although studies incorporating a greater number of mice with higher serum AP levels are required to establish significance. If TNAP has a significant role in the etiology of craniosynostosis, TNAP enzyme replacement therapies currently used to treat mineralization defects in hypophosphatasia patients (25) could be used to prevent and/or treat craniosynostosis.

ACKNOWLEDGEMENTS

The authors thank Dr. Jose Luis Millán for providing the lentivirus utilized in these studies. This work was supported by grant DE021082 from the National Institute of Dental and Craniofacial Research and by The Hartwell Foundation.

References

1. Rasmussen SA, Yazdy MM, Frías JL, Honein MA. Priorities for public health research on craniosynostosis: summary and recommendations from a Centers for Disease Control and Prevention-sponsored meeting. Am J Med Genet A. 2008; 146A(2):149–158. [PubMed: 18080327]

2. Baird LC, Gonda D, Cohen SR, Evers LH, Lefloch N, Levy ML, et al. Craniofacial reconstruction as a treatment for elevated intracranial pressure. Childs Nerv Syst. 2011; 28(3):411–418. [PubMed: 22068642]

3. Warren SM, Proctor MR, Bartlett SP, Blount JP, Buchman SR, Burnett W, et al. Parameters of care for craniosynostosis: craniofacial and neurologic surgery perspectives. Plast Reconstr Surg. 2012; 129(3):731–737. [PubMed: 22373978]

4. Hatch NE. FGF signaling in craniofacial biological control and pathological craniofacial development. Crit Rev Eukaryot Gene Expr. 2010; 20(4):295–311. [PubMed: 21395503]

5. Eswarakumar VP, Horowitz MC, Locklin R, Morriss-Kay GM, Lonai P. A gain-of-function mutation of Fgfr2c demonstrates the roles of this receptor variant in osteogenesis. Proc Natl Acad Sci U S A. 2004; 101(34):12555–12560. [PubMed: 15316116]

6. Perlyn CA, DeLeon VB, Babbs C, Govier D, Burell L, Darvann T, et al. The craniofacial phenotype of the Crouzon mouse: analysis of a model for syndromic craniosynostosis using three-dimensional MicroCT. Cleft Palate Craniofac J. 2006; 43(6):740. [PubMed: 17105336]

7. Liu J, Nam HK, Wang E, Hatch NE. Further analysis of the Crouzon mouse: effects of the FGFR2(C342Y) mutation are cranial bone-dependent. Calcif TissueInt. 2013; 92(5):451–466.

8. Chen L, Li D, Li C, Engel A, Deng CX. A Ser252Trp [corrected] substitution in mouse fibroblast growth factor receptor 2 (Fgfr2) results in craniosynostosis. Bone. 2003; 33(2):169–178. [PubMed: 14499350]

9. Yin L, Du X, Li C, Xu X, Chen Z, Su N, et al. A Pro253Arg mutation in fibroblast growth factor receptor 2 (Fgfr2) causes skeleton malformation mimicking human Apert syndrome by affecting both chondrogenesis and osteogenesis. Bone. 2008; 42(4):631–643. [PubMed: 18242159]

10. Twigg SR, Healy C, Babbs C, Sharpe JA, Wood WG, Sharpe PT, et al. Skeletal analysis of the Fgfr3(P244R) mouse, a genetic model for the Muenke craniosynostosis syndrome. Dev Dyn. 2009; 238(2):331–342. [PubMed: 19086028]

11. Murshed M, Harmery D, Millan JL, McKee MD, Karsenty G. Unique coexpression I osteoblasts of broadly expressed genes accounts for the spatial restriction of ECM mineralization to bone. Genes and Dev. 2009; 19:1093–1104. [PubMed: 15833911]

12. Johnson K, Moffa A, Chen Y, Pritzker K, Goding J, Terkeltaub R. Matrix vesicle plasma cell membrane glycoprotein-1 regulates mineralization by murine osteoblastic MC3T3 cells. J Bone Miner Res. 1999; 14:883–892. [PubMed: 10352096]

13. Johnson KA, Hessle L, Vaingankar S, Wennberg C, Mauro S, Narisawa S, et al. Osteoblast tissue-nonspecific alkaline phosphatase antagonizes and regulates PC-1. Am J Physiol Regul Integr Comp Physiol. 2000; 279:R1365–R1377. [PubMed: 11004006]

14. Hessle L, Johnson KA, Anderson HC, Narisawa S, Sali A, Goding JW, et al. Tissue-nonspecific alkaline phosphatase and plasma cell membrane glycoprotein-1 are central antagonistic regulators of bone mineralization. Proc Natl Acad Sci. 2002; 99:9445–9449. [PubMed: 12082181]

15. Register TC, Wuthier RE. Effect of pyrophosphate and two diphosphonates on 45Ca and 32Pi uptake and mineralization by matrix vesicle-enriched fractions and by hydroxyapatite. Bone. 1985; 6:307–312. [PubMed: 3006731]

16. Johnson K, Pritzker K, Goding J, Terkeltaub R. The nucleoside triphosphate pyrophosphohydrolase isozyme PC-1 directly promotes cartilage calcification through chondrocyte apoptosis and increased calcium precipitation by mineralizing vesicles. J Rheumatol. 2001; 8:2681–2691. [PubMed: 11764218]

17. Johnson K, Goding J, VanEtten D, Sali A, Hu S, Farley D, et al. Linked deficiencies in extracellular PPi and osteopontin mediate pathologic calcification associated with defective PC-1 and ANK expression . J Bone Min Res. 2003; 1:994–1004.

18. Thouverey C, Bechkoff G, Pikula S, Buchet R. Inorganic pyrophosphate as a regulator of hydroxyapatite or calcium pyrophosphate dihydrate mineral deposition by matrix vesicles. Osteoarthritis Cartilage. 2009; 17(1):64–72. [PubMed: 18603452]

19. Beck GR Jr, Zerler B, Moran E. Phosphate is a specific signal for induction of osteopontin gene expression. Proc Natl Acad Sci U S A. 2000; 97(15):8352–8357. [PubMed: 10890885]

20. Polewski MD, Johnson KA, Foster M, Millán JL, Terkeltaub R. Inorganic pyrophosphatase induces type I collagen in osteoblasts. Bone. 2010; 46(1):81–90. [PubMed: 19733704]

21. Nam HK, Liu J, Li Y, Kragor A, Hatch NE. Ectonucleotide pyrophosphatase/phosphodiesterase-1 (ENPP1) protein regulates osteoblast differentiation. J Biol Chem. 2011; 286(45):39059–39071. [PubMed: 21930712]
22. Collmann H, Mornet E, Gattenlöhner S, Beck C, Girschick H. Neurosurgical aspects of childhood hypophosphatasia. Childs Nerv Syst. 2009; 25(2):217–223. [PubMed: 18769927]
23. Whyte MP. Physiological role of alkaline phosphatase explored in hypophosphatasia. Ann N Y Acad Sci. 2010; 1192:190–200. [PubMed: 20392236]
24. Mornet E. Hypophosphatasia. Orphanet J Rare Dis. 2007; 2:40. [PubMed: 17916236]
25. Whyte MP, Greenberg CR, Salman NJ, Bober MB, McAlister WH, Wenkert D, et al. Enzyme-replacement therapy in life-threatening hypophosphatasia. N Engl J Med. 2012; 366(10):904–913. [PubMed: 22397652]
26. Hatch NE, Nociti F, Swanson E, Bothwell M, Somerman M. FGF2 alters expression of the pyrophosphate/phosphate regulating proteins, PC-1, ANK and TNAP, in the calvarial osteoblastic cell line, MC3T3E1(C4). Connect Tissue Res. 2005; 46(4–5):184–192. [PubMed: 16546821]
27. Hatch NE, Li Y, Franceschi RT. FGF2 stimulation of the pyrophosphate-generating enzyme, PC-1, in pre-osteoblast cells is mediated by RUNX2. J Bone Miner Res. 2009; 24(4):652–662. [PubMed: 19049325]
28. Yamamoto S, Orimo H, Matsumoto T, Iijima O, Narisawa S, Maeda T, et al. Prolonged survival and phenotypic correction of Akp2(−/−) hypophosphatasia mice by lentiviral gene therapy. J Bone Miner Res. 2011; 26(1):135–142. [PubMed: 20687159]
29. Nishioka T, Tomatsu S, Gutierrez MA, Miyamoto K, Trandafirescu GG, Lopez PL, et al. Enhancement of drug delivery to bone: characterization of human tissue-nonspecific alkaline phosphatase tagged with an acidic oligopeptide. Mol Genet Metab. 2006; 88(3):244–255. [PubMed: 16616566]
30. Richtsmeier JT, Baxter LL, Reeves RH. Parallels of craniofacial maldevelopment in Down syndrome and Ts65Dn mice. Dev Dyn. 2000; 217(2):137–145. [PubMed: 10706138]
31. Lele, S.; Richtsmeier, JT. An invariant approach to statistical analysis of shapes. Boca Raton, FL: Chapman & Hall/CRC; 2001.
32. Millan JL, Narisawa S, Lemire I, Loisel TP, Boileau G, Leonard P, et al. Enzyme replacement therapy for murine hypophosphatasia. J Bone Miner Res. 2008; 23:777–787. [PubMed: 18086009]
33. Yadav MC, Lemire I, Leonard P, Boileau G, Blond L, Beliveau M, et al. Dose response of bone-targeted enzyme replacement for murine hypophosphatasia. Bone. 2011; 49(2):250–256. [PubMed: 21458605]

CLINICAL RELEVANCE

Craniosynostosis occurs in association with activating mutations in fibroblast growth factor receptors and inactivating mutations in TNAP (tissue-nonspecific alkaline phosphatase). Because FGF signaling regulates TNAP expression and because TNAP is an established mediator of tissue mineralization, we hypothesize that dysregulation of TNAP downstream of mutant FGF receptors leads to craniosynostosis and associated abnormalities. To test this hypothesis, here we injected Crouzon mice with lentivirus expressing TNAP. While variable, our results suggest that delivery of TNAP may diminish the degree of craniofacial skeletal malformation seen in the $FGFR2^{C342Y/+}$ mouse model of Crouzon craniosynostosis.

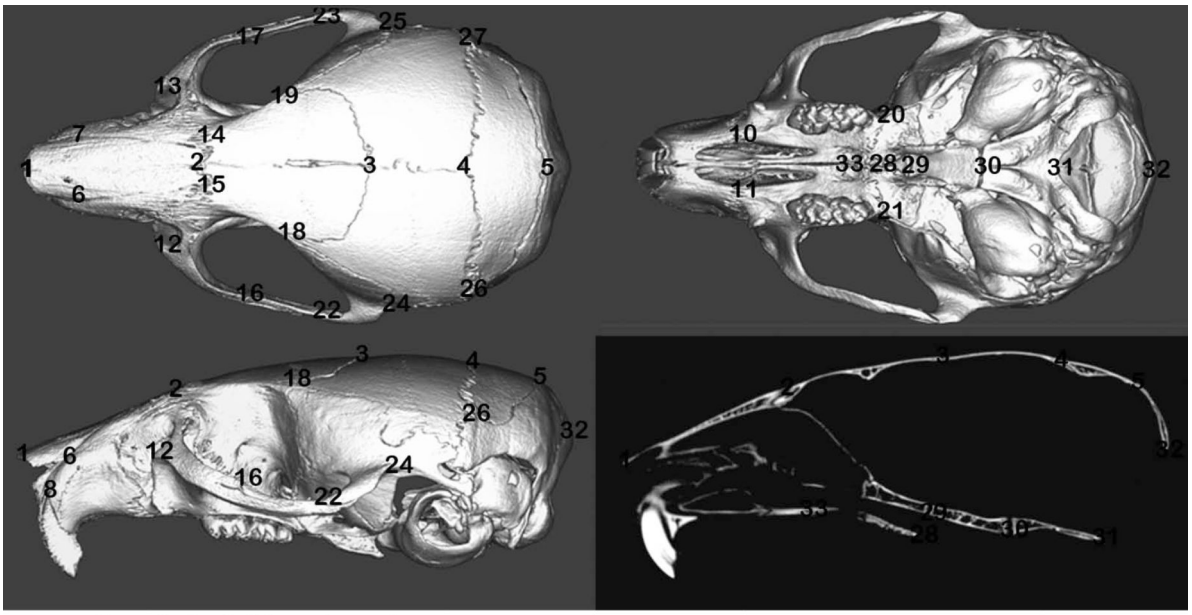

Craniofacial Landmarks

1	nasale, intersection of nasal bones, rostral point
2	nasion, intersection of nasal bones, caudal point
3	bregma, intersection of frontal bones and parietal bones at midline
4	pari, intersection of parietal and anterior aspect of interparietal bones at midline
5	paro, intersection of interparietal and occipital bones at the midline
6,7	anterior-most point at intersection of premaxillae and nasal bones
8,9	center of alveolar ridge over maxillary incisor
10,11	most inferior point on premaxilla-maxilla suture
12,13	anterior notch on frontal process lateral to infraorbital fissure
14,14	intersection of frontal process of maxilla with frontal and lacrimal bones
16,17	intersection of zygomatic process of maxilla with zygoma, superior surface
18,19	frontal-squamosal intersection at temporal crest
20,21	intersection of maxilla and sphenoid on inferior alveolar ridge
22,23	intersection of zygoma with zygomatic process of temporal, superior aspect
24,25	joining of squamosal body to zygomatic process of squamous portion of temporal bone
26,27	intersection of parietal, temporal and occipital bones
28	PNS - posterior nasal spine
29	ISS – intersphenoidal suture, inferior point
30	SOS – spheno-occipital suture, inferior point
31	basion
32	opisthion
33	posterior palatine fissure

Landmarks with two numbers denote bilateral structures.

Figure 1. Three-dimensional craniofacial skeletal landmarks

Location and description of thirty-three craniofacial skeletal landmarks placed on micro CT scans of mouse skulls are indicated.

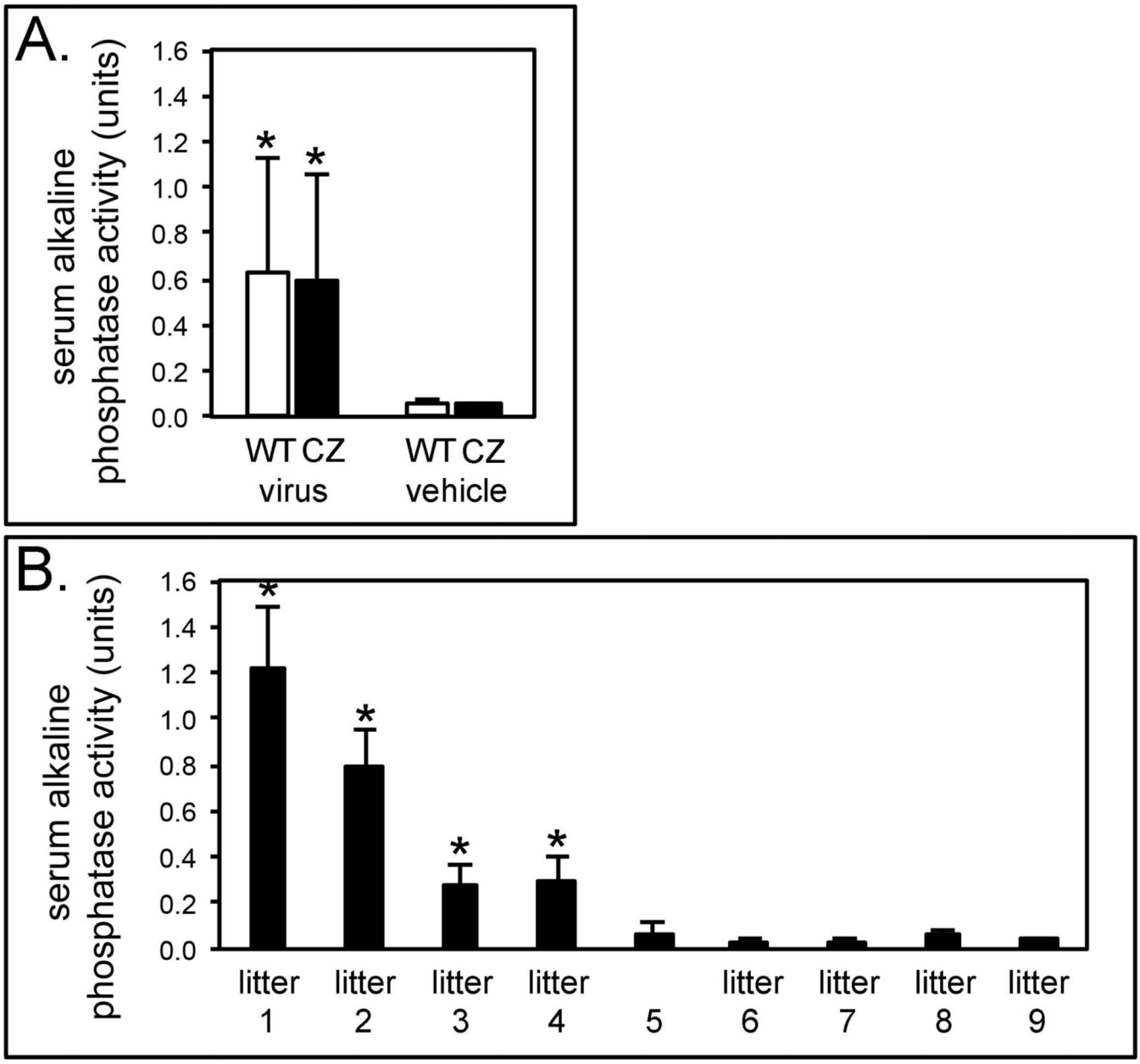

Figure 2. Serum alkaline phosphatase enzyme activity levels by genotype, treatment group and litter of mice

A) Serum alkaline phosphatase enzyme activity levels of TNAP lentivirus injected vs. vehicle injected mice. *p < .05 vs. vehicle injected mice. WT = wild type mice, CZ = Crouzon mice, virus = TNAP lentivirus injected, vehicle = vehicle injected. **B)** Serum alkaline phosphatase enzyme activity levels by litter of mice. Litters 1–5 were injected with the TNAP lentivirus. Litters 6–9 were injected with vehicle. *indicates significant difference between TNAP lentivirus injected values of each litter, compared to all vehicle injected mice, where p < .05.

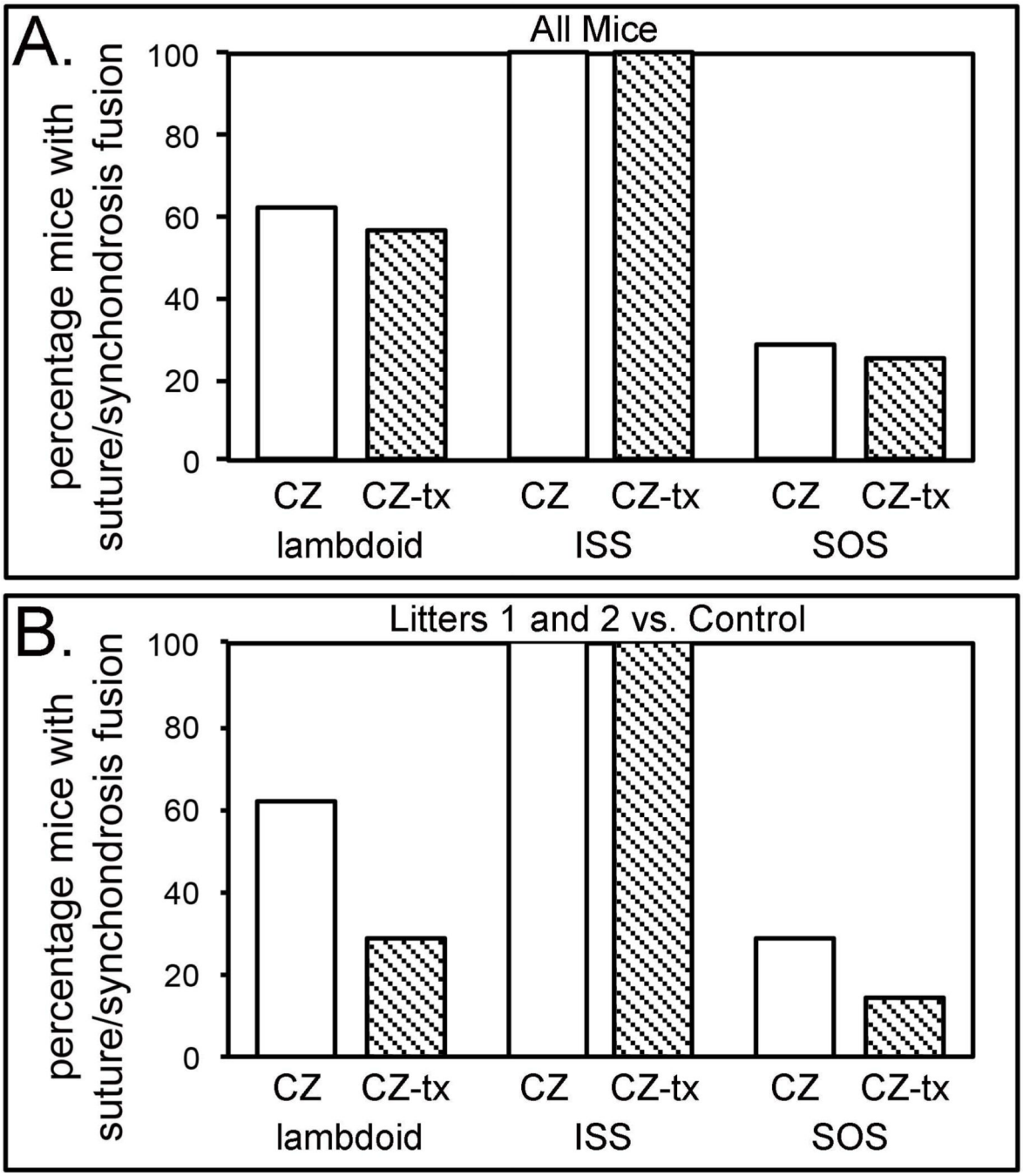

Figure 3. Percentage of TNAP lentivirus injected vs. vehicle injected Crouzon mice with cranial suture and synchondrosis fusion

A) Fusion percentages of vehicle and TNAP lentivirus injected Crouzon mice, combining all litters of mice (litters 1–5 for TNAP lentivirus injected, litters 6–9 for vehicle injected). **B)** Fusion percentages of vehicle injected and only litters 1 and 2 of TNAP lentivirus injected Crouzon mice. CZ = Crouzon vehicle injected, CZ-tx = Crouzon TNAP lentivirus injected, ISS = intersphenoidal synchondrosis, SOS = sphenoccipital synchondrosis, control = vehicle injected.

Table 1

Body Weight and Length as Influenced by AP level, genotype and gender.

	Overall R^2 with p value	Parameters	Coefficient (β) with p value	95% Confidence Intervals	
				lower bound	upper bound
Body Weight (g)	R^2 = .519 p < .0001	intercept	14.04 p < .0001 *	13.20	14.88
		AP level	−1.42 p = .004*	−2.36	−0.47
		Genotype (Cz)	−2.88 p < .0001 *	−3.70	−2.08
		Gender (F)	−0.55 p = .12	−1.38	.28
Body Length (mm)	R^2 = .395 p < .0001	intercept	78.38 p < .0001 *	75.73	81.04
		AP level	−4.547 p = .003*	−7.53	−1.56
		Genotype (Cz)	−6.513 p < .0001 *	−9.08	−3.95
		Gender (F)	−2.175 p = .10	−4.80	0.46

* Indicates statistical significance.

Table 2

Cranial suture and synchondrosis fusion as Influenced by Alkaline Phosphatase (AP) level.

Suture or Synchondrosis	Parameter	Coefficient (β) with p value	95% Confidence Intervals		Odds Ratio for Fusion
			lower bound	upper bound	
Lambdoid	AP level	−1.85 p < .068	0.02	1.14	84.2%
Spheno-occipital Syndondrosis	AP level	−0.54 p < .602	.08	4.4	41.7%

Table 3

Craniofacial Morphologic Analysis.

Landmark Subset	Number of Landmarks in Subset	Form Comparison p value
superior surface	9	.080
inferior surface	9	.023*
lateral surface	9	.657
cranial vault vertical	7	.014*
cranial vault transverse	7	.496

* Indicates statistical significance between treatment groups.